Echo Reduction Properties of Fast Non-Redundant Planar NF Sampling Methodologies

F. D'Agostino[1], F. Ferrara[1], C. Gennarelli[1], R. Guerriero[1], M.A. Saporetti[2], F.Saccardi[2], L.J. Foged[2], D. Trenta[3]

[1]D.I.In. - Università di Salerno, via Giovanni Paolo II, 132, - 84084 Fisciano (SA), Italy, (fdagostino, flferrara, cgennarelli, rguerriero)@unisa.it

[2]Microwave Vision Italy SRL, Via dei Castelli Romani,59, Pomezia (RM), Italy, (maria.saporetti, francesco.saccardi, lars.foged)@ mvg-world.com

[3] European Space Agency, ESTEC, The Netherlands, Damiano.Trenta@esa.int

***Abstract*—The optimal sampling interpolation expansion is employed in near field measurements to reconstruct the field at any point of the observation surface starting from a non-redundant scanning scheme [1]-[3]. Such schemes allow faster measurements than classical Nyquist-compliant acquisitions. The methodology has no accuracy loss and has been validated at different bands and with different antennas [5], [6]. As the metrology restricts the source region to a surface conformal to the measured antenna, it intrinsically acts as low-pass spatial filter and thus possess echo reduction properties [7].**

In this paper, the echo reduction benefits of the optimal sampling interpolation expansion applied to Planar Near Field measurements is investigated for the first time. A standard gain horn, MVG SGH4000 has been measured at V-band in an environment with controlled echoes. The results obtained with non-redundant methodology are compared against classical measurements post-processed with standard echo reduction techniques [8].

***Index Terms*—antennas, planar measurements, echo reduction, post-processing, non-redundant sampling, optimal interpolation functions.**

I. INTRODUCTION

Much faster measurements than standard Near Field Nyquist-compliant [4] scanning can be performed implementing non-canonical sampling schemes based on the application of the non-redundant sampling representations of the electromagnetic (EM) fields [5] to represent the voltage measured by a nondirective probe. For planar measurements, this is accomplished by the Planar Wide-Mesh scanning (PWMS) ([1]-[2][2]), while, for the spherical measurements, the sampling points are arranged on a non-redundant raster grid [3]. The methodology is without any loss of accuracy and has been validated at different bands and with different kinds of antennas under test (AUTs) [5].

Starting from non-redundant measurements, the voltage at any point on the measurement plane or sphere can be efficiently reconstructed by means of two-dimensional optimal sampling interpolation (OSI) expansions. An intrinsic characteristic of these interpolation expansions is to act as a low-pass filter: the spectral content of noise and echoes at the spatial frequencies higher than the antenna spatial bandwidth is cut away.

In this paper, we investigate and experimentally verify, for the first time, the echo reduction properties of the OSI expansions. The verification has been carried out by measuring an MVG SGH4000 standard gain horn at 48GHz, using a 6 axes Staubli robot [6]. The measurement scenario is characterized by echo and stray signals originated from signals scattered by the 6 axes Staubli robot.

In order to mitigate the errors arising from the presence of echo and/or stray signals, the Far Field reconstructed with classical Near Field to Far Field (NFFF) transformation has been post-processed with spatial filtering implemented by the MV-Echo software [7]-[11]. The original far field and the filtered one have been compared with results obtained by the non-redundant methodology.

The paper is organized as follows: in Par. II, the echo reduction properties of non-canonical scanning and irregular sampling approach are presented from a theoretical point of view. Par. III describes the details of the experimental verifications. The results are shown in terms of patterns and Equivalent Noise Level. Finally, the conclusions and future activities are summarized in Par. IV.

II. ECHO REDUCTION PROPERTIES OF NON-REDUNDANT SAMPLING METHODOLOGIES

For reader's convenience, the filtering properties of the OSI expansions are highlighted in the following in the case of the non-conventional plane-rectangular scanning, named PWMS. In any case, these characteristics are common to all the NF scanning techniques based on the non-redundant representations of the EM fields and adopting the OSI schemes to reconstruct the voltage acquired by a non-directive probe at any point of the observation surface.

Let us suppose that the considered non-directive probe scans a plane d away from a quasi-planar AUT and adopt the rectangular coordinate system (x, y, z), with the origin O at the AUT aperture centre, and the spherical one (r, ϑ, φ) to denote any observation point. Moreover, let us also introduce the coordinate system (x', y', z') with the origin O' on the plane to specify a point P on the scanning plane (see Fig. 1). According to the non-redundant sampling representations [4], the AUT must be considered as contained in a proper convex

rotational surface Σ (an oblate ellipsoid or a two-bowls) fitting well its geometry, an optimal parameter ξ has to be employed for describing a curve C on the plane and a suitable phase factor $e^{-j\gamma(\xi)}$ must be singled out from the acquired voltage. The so obtained "reduced voltage" $\tilde{V}(\xi,\eta)e^{j\gamma(\xi)}$, where V denotes the voltage V_y or V_x acquired by the probe or by the rotated probe, can be closely approximated by a function spatially bandlimited to $\chi' W_\xi$ [2], [3]. When the curve C is a radial line, as the x'-, or y'- axis, the bandwidth W_ξ, the parameter ξ, and the phase function γ are given by

$$W_\xi = \beta\ell\,; \qquad \xi = (\pi/\ell)\left[\quad + s_1' + s_2'\right] \tag{1}$$

$$\gamma = (\beta/2)\left[R_1 + R_2 + s_1' - s_2'\right] \tag{2}$$

where β is the free-space wavenumber, ℓ the length of C', intersection curve between the surface Σ and the meridian plane through the observation point P, $s_{1,2}'$ the arclength coordinates of the two tangency points $P_{1,2}$ on C', and $R_{1,2}$ the distances from P to $P_{1,2}$. The explicit expressions of ℓ, $R_{1,2}$, and $s_{1,2}'$ depend on the particular choice of the surface Σ enclosing the AUT and change accordingly [2], [3].

It can be easily recognized [2], [3] that the same parameterization $x' = x'(\xi)$, or $y' = y'(\eta)$ must be mandatorily employed to describe all lines parallel to the x' or y' axis in order to allow the factorization of the two-dimensional interpolation algorithm into one-dimensional OSI expansions along lines. In other words, the samples spacing on all lines parallel to the x' or y' axis coincides with that relevant to the x' or y' axis, respectively (see Fig. 1). This corresponds to use a parameter that does not make constant the local bandwidth, but, since this last is always less or equal than W_ξ, the number of samples is greater than that required by a rigorous application of a non-redundant sampling representation and no further representation error is introduced [2]. Therefore, the raster grid in the PWMS has meshes which become larger and larger as their distance from the centre of the scanning plane increases. As regards the phase function γ, it can be determined [2], [3] by means of (2). Namely, it depends only on the observation point P and is the same that would be adopted in the interpolation along the radial line passing through P.

Being now possible to represent the voltage acquired by the considered probe in terms of its samples, strictly related to the AUT spatial bandwidth, it is possible to resort to the following effective two-dimensional OSI algorithm, in order to accurately reconstruct the probe voltage at a point $P(x', y')$ on the measurement plane:

$$V_{x,y}(\xi(x'),\eta(y')) = e^{-j\gamma(x',y')} \sum_{m=m_0-p+1}^{m_0+p} \left\{ H(\eta,\eta_m,\bar{\eta},N,N'') \cdot \right.$$

$$\left. \sum_{n=n_0-q+1}^{n_0+q} V_{x,y}(\xi_n,\eta_m) e^{j\gamma(x_n',y_m')} H(\xi,\xi_n,\bar{\xi},N,N'') \right\} \tag{3}$$

where $n_0 = \lfloor \xi/\Delta\xi \rfloor$, $m_0 = \lfloor \eta/\Delta\eta \rfloor$,

$$\xi_n = n\Delta\xi = 2\pi n/(2N''+1)\,; \quad \eta_m = m\Delta\eta = m\Delta\xi \tag{4}$$

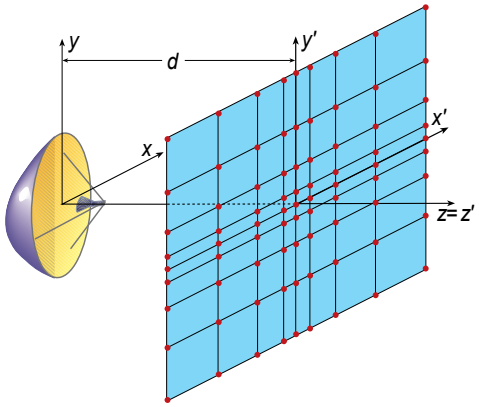

Fig. 1. Planar wide-mesh scanning

$$N'' = \lfloor \chi N' \rfloor + 1\,; \quad N' = \lfloor \chi' W_\xi \rfloor + 1\,; \quad W_\eta = W_\xi\,; \tag{5}$$

$$N = N'' - N'\,; \quad \bar{\xi} = q\Delta\xi\,; \quad \bar{\eta} = p\Delta\eta \tag{6}$$

$\lfloor x \rfloor$ denotes the integer part of x, and χ is the OSI oversampling factor required to control the truncation error [4].

These OSI expansions are of central type and, accordingly, make use only of a reduced number of NF samples around the given output point, $2q$, say, that along the sampling lines parallel to x' axis and $2p$ that along the lines parallel to y' one. Their capability to minimize the truncation error for a reduced number of retained samples depends on the fact that the OSI kernel $H(\alpha,\alpha_i,\bar{\alpha},L,L'')$ is the product of the Direchlet function $D_{L''}(\alpha)$, the standard interpolation function for a closed domain, by the Tschebyscheff sampling window $\Omega_L(\alpha,\bar{\alpha})$, a weight function able to accelerate the convergence of the OSI expansion [4].

When reconstructing the NF data along the sampling lines of the standard raster grid, their behaviour will appear smoother, as compared with that corresponding to the directly measured ones. This is due to the filtering property of the OSI kernel, that has the capability to reject the spatial harmonics of the noise and residual reflections exceeding the AUT spatial bandwidth. In any case, another beneficial effect results from the adoption of the OSI scheme as compared with the use of the cardinal series (CS) representation, which should represent in such a case the natural choice, from the information theory viewpoint. In fact, this last, while completely satisfactory from the accuracy point of view, has the drawback to not prevent the propagation of the errors affecting the data from high to low voltage regions, due to the slow decay of the involved interpolation functions. In particular, provided that, in any practical instance, we are well above the noise level, the measured results are usually affected by a (approximately) constant relative, not absolute, error, so that the absolute error corresponding to the highest voltage values can be relatively large. This error is spread out by the CS sampling functions without a severe attenuation, and this gives rise to a remarkable relative error in the zones where the voltage level is low. This effect is avoided when adopting the OSI scheme, since only the NF samples in the neighbourhood of any given output point are considered.

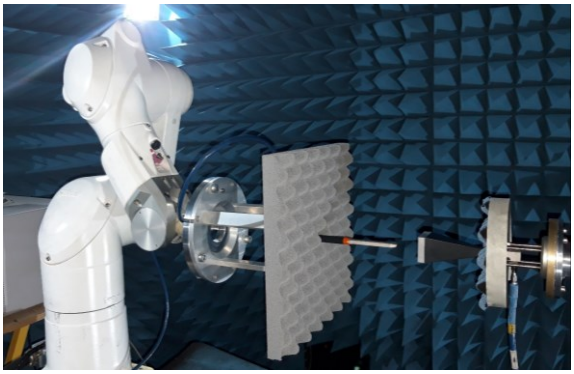

Fig. 2. MVG SGH4000 in the planar NF measurement system with 6-axes Staubli robot.

III. EXPERIMENTAL VERIFICATIONS

Experimental verifications have been performed by measuring a MVG SGH4000 standard gain horn antenna in a PNF measurement system emulated by a 6 axes Staubli robot, as shown in Fig. 2. The SGH4000 is characterized by stable gain with frequency and low return loss/VSWR and is based on a stiff and robust mechanical design, precision machined with accurate polarization alignment. The scan plane size is 40x40 cm and the AUT-to-Scanner distance is 4 cm.

Measurements have been performed using both a standard grid with λ/2-spacings between the NF acquisition points and the PWMS one. In such a configuration, at 48 GHz, the use of the PWMS allows one to reduce the number of NF samples with a factor equals to 12 [6].

As underlined in Fig. 3, the robot structure scatters signals that produce echo and stray signals in the measurement environment. This is evident by analyzing FF patterns computed using a standard Planar NFFF transformation, including probe corrections for the used MVG OEW330 (WR229) open ended waveguide. The echo and stray signals have been successfully mitigated applying a spatial filtering implemented by the MV-Echo software ([7]-[10]). The spatial filtering implemented within the MV-Echo software is based on the expansion of the measured field over a set of orthogonal spherical wave expansion (SWE) modes [11]. Such an expansion is then combined with a modal filtering based on the knowledge of the physical extent of the AUT).

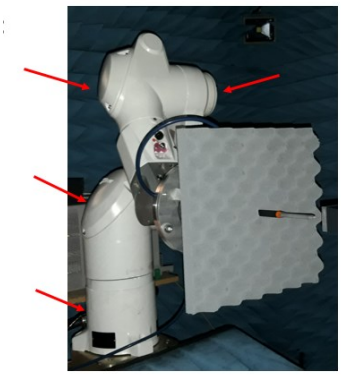

Fig. 3. 6-axis Staubli robot with indication of the scattering sources from the uncovered parts of the robot body.

The original far field and the spatially filtered one have been compared with the results obtained by using the non-redundant methodology. The comparison shows the pattern obtained by the classical NFFF transformation (blue curve), the spatially filtered classical NFFF transformation (red curve) and the non-redundant PWMS methodology (yellow curve).

Fig. 4, Fig. 6 and Fig. 8 show the gain pattern, respectively, at phi=0°, phi=45°, phi=90° for the co-polar and cross-polar FF components at 48 GHz. The shadowed areas in the plots below represent the regions outside the validity angle, computed taking into account the geometrical constraints and equal to 78°.

The presence of echo and stray signal in the measurement scenario is evident on the disagreement of the cross-polar components and of the main beam, as visible in the zoom of Fig. 5, Fig. 7 and Fig. 9 respectively for the cuts at phi=0°, phi=45° and phi=90°.

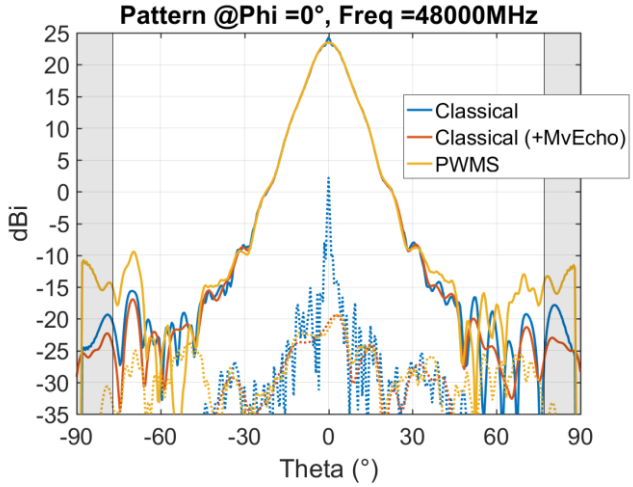

Fig. 4. SGH4000 gain pattern @48GHz at phi=0°cut, copolar (solid curve) and crosspolar (dashed curve) components for classical measurement (blue line), spatially filtered classical measurements (red curve) and PWMS (yellow line).

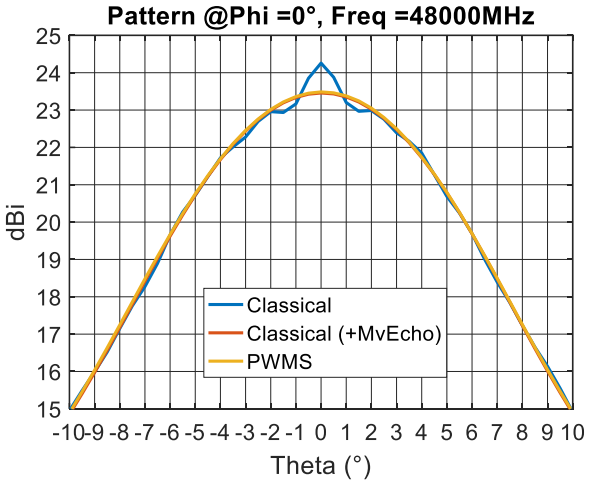

Fig. 5. Zoom on the main beam of SGH4000 gain pattern @48GHz at phi=0°cut, copolar component for classical measurement (blue line), spatially filtered classical measurements (red curve) and PWMS (yellow line).

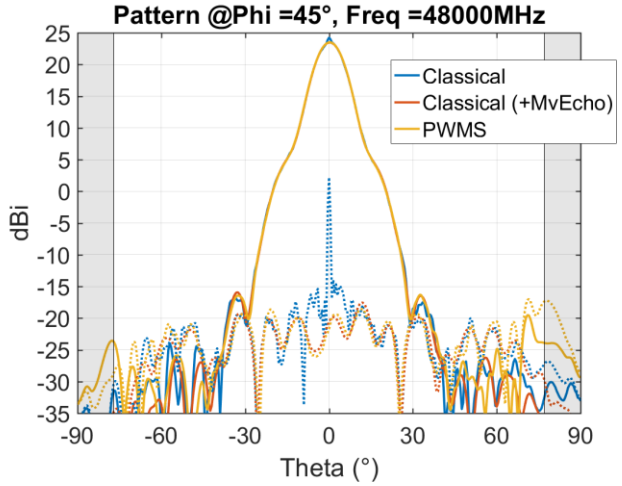

Fig. 6. SGH4000 gain pattern @48GHz at phi=45°cut, copolar (solid curve) and crosspolar (dashed curve) components for classical measurement (blue line), spatially filtered classical measurements (red curve) and PWMS (yellow line).

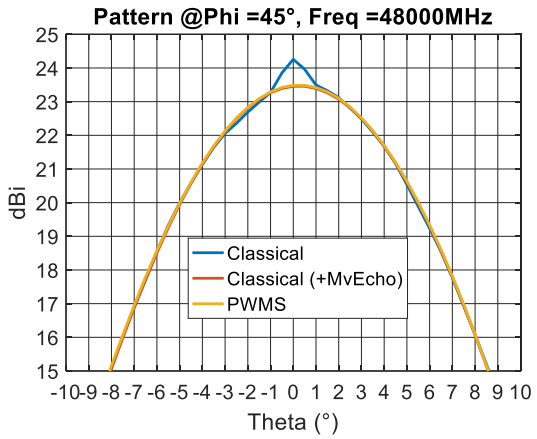

Fig. 7. Zoom on the main beam of SGH4000 gain pattern @48GHz at phi=45°cut, copolar component for classical measurement (blue line), spatially filtered classical measurements (red curve) and PWMS (yellow line).

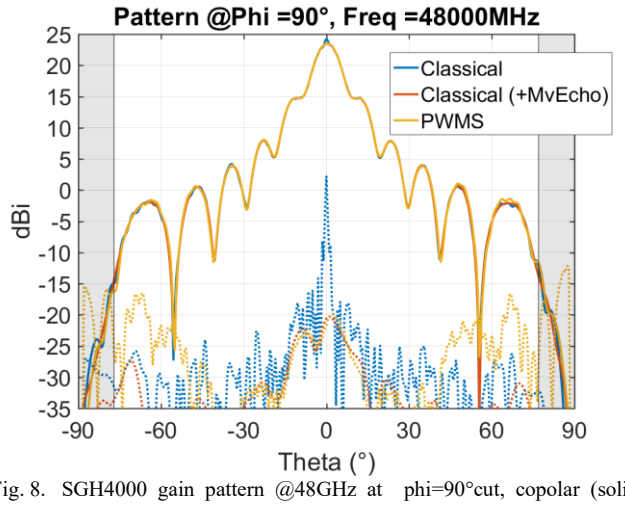

Fig. 8. SGH4000 gain pattern @48GHz at phi=90°cut, copolar (solid curve) and crosspolar (dashed curve) components for classical measurement (blue line), spatially filtered classical measurements (red curve) and PWMS (yellow line).

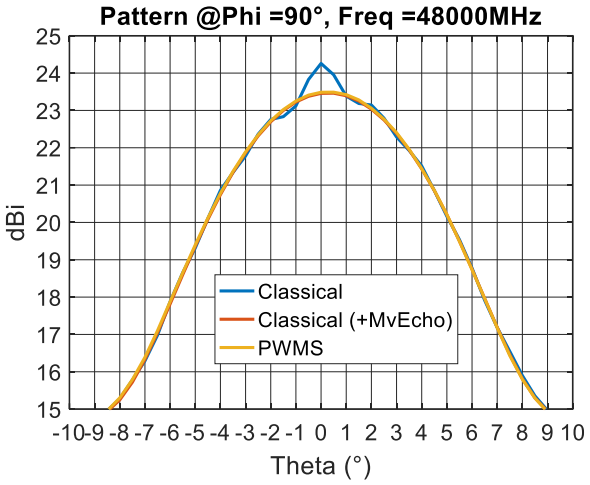

Fig. 9. Zoom on the main beam of SGH4000 gain pattern @48GHz at phi=90°cut, copolar component for classical measurement (blue line), spatially filtered classical measurements (red curve) and PWMS (yellow line).

As expected, the spatial filtering operated by MVEcho mitigates the effects of the echo and stray signals. The PWMS far field does not need any post-processing implanting echo reduction, since, as already underlined, the interpolation acts as low-pass filtering removing the spectral content of the noise at the spatial frequencies higher than the antenna spatial bandwidth.

The correlation between the patterns can be expressed thorough the Equivalent Noise Level, through which all the deviations wrt to a reference are converted into a single noise [12]. In the analysis presented in the following, classical measurements post-processed with spatial filtering have been used as reference since the spatial filtering performed in MV Echo has been already validated in previous activities ([7]-[10]). TABLE I. shows the Equivalent Noise Level (ENL) of the Classical Nyquist compliant measurement and the ENL of the fast optimal sampling methodology computed on all cuts, in a cone with θ ranging in the validity angle and considering copolar and crosspolar components.

TABLE I. EQUIVALENT NOISE LEVEL

Methodology	***ENL [dB]***
Clasical Nyquist-compliant	-41.00
PWMS	-55.38

As can be inferred, MV Echo compensates for the noise on the main beam of the copolar and on the crosspolar components. The spatially filtered classical far field has a very good agreement with the PWMS, confirming the spatial filtering and echo reduction properties.

IV. Conclusions

Optimal sampling interpolation expansions, employed for faster measurements than classical Nyquist-compliant acquisitions, intrinsically have spatial low-pass filtering. The spectral content of the noise at the spatial frequencies higher than the antenna spatial bandwidth is cut away. These spatial filtering and echo reduction properties have been investigated and verified for the first time at V-band using an MVG SGH4000 standard gain horn in a PNF measurement system emulated by a 6 axes Staubli robot. The measurement environment was characterized by scatters signals producing echo and stray signals. The gain patterns obtained with the non-redundant methodology have been compared against classical measurements and classical measurements post-processed with spatial filtering, implemented with the MV-Echo SW. The filtering properties of the non-redundant methodology are confirmed by the very good visual agreement shown with classical measurements post-processed with spatial filtering. This is further confirmed by the very low ENL of -55dB.

Acknowledgment

The activities reported in this paper have been partly supported through ESA project "Measurement Methodology For Fast Antenna Testing" and through ARTES by the Italian Space Agency [13].

References

[1] F. Ferrara, C. Gennarelli, R. Guerriero, G. Riccio, C. Savarese, "An efficient near-field to far-field transformation using the planar wide-mesh scanning," Jour. Electromagn. Waves Appl., vol. 21, no. 3, pp. 341-357, 2007.

[2] F. D'Agostino, I. De Colibus, F. Ferrara, C. Gennarelli, R. Guerriero, M. Migliozzi, "Far-field pattern reconstruction from near-field data collected via a nonconventional plane-rectangular scanning: experimental testing," Int. Jour. Antennas Prop., vol. 2014, Art. no. 763687, pp. 1-9, 2014.

[3] F. D'Agostino, F. Ferrara, C. Gennarelli, R. Guerriero, M. Migliozzi, "Effective antenna modellings for NF–FF transformations with spherical scanning using the minimum number of data," Int. Jour. Antennas Prop., vol. 2011, ID 936781, 11 pages.

[4] O.M. Bucci, C. Gennarelli, C. Savarese, "Representation of electromagnetic fields over arbitrary surfaces by a finite and nonredundant number of samples," IEEE Trans. Antennas Prop., vol. 46, pp. 351-359, March 1998.

[5] F. D'Agostino, F. Ferrara, C. Gennarelli, R. Guerriero, M. A.Saporetti, F. Saccardi, L. J. Foged, D. Trenta, "Fast measurement methodology for near field satellite testing," Proc. of EUCAP 2019, Krakow, Poland, Apr. 2019.

[6] M. A.Saporetti, F. Saccardi, L. J. Foged, F. D'Agostino, F. Ferrara, C. Gennarelli, R. Guerriero, "Experimental Validation of Minimum Redundancy Scanning Schemes in PNF Measurements at V band" AMTA Symposium, October 2019, San Diego, California USA.

[7] IEEE std 1720 "Recommended Practice for Near-Field Antenna Measurements.

[8] L. J. Foged, L. Scialacqua, F. Mioc, F. Saccardi, P. O. Iversen, L. Shmidov, R. Braun, J. L. Araque Quijano, G. Vecchi,"Echo Suppresion by Spatial Filtering Techniques in Advanced Planar and Spherical NF Antenna Measurements", AMTA Symposium, October 2012, Seattle, Washington, USA.

[9] L. Salghetti Drioli, L.J. Foged, F. Saccardi, F. Mioc, L. Scialacqua, S. Burgos, T. Kozan, P.O. Iversen L. Shmidov, R. Braun, "Investigation of Echo Suppression Efficiency in Spacecrafts Near Field Measurement Scenarios" AMTA, 12-17 October 2014, Tucson, Arizona, USA.

[10] Manuel José López Morales, Francesco Saccardi, Manuel Sierra Castañer, Lars J. Foged, "Comparison of Echo Reduction Techniques for One-Single Cut Antenna Measurements" EuCAP, Davos, Switzerland, 10-15 April 2016.

[11] J. E. Hansen, Spherical Near-Field Antenna Measurements, Peter Peregrinus Ltd. On behalf of IEE, London, United Kingdom, 1988.

[12] M.A.Saporetti, L.J. Foged, F. las Heras, A. A. Alexandridis, C. López , I Y. Kurdi, M. Sierra Castañer, International Facility Comparison Campaign at L/C Band Frequencies, AMTA 2017.

[13] ESA Contract No. 4000121164/17/UK/ND, ARTES "Measurement Methodology For Fast Antenna Testing".